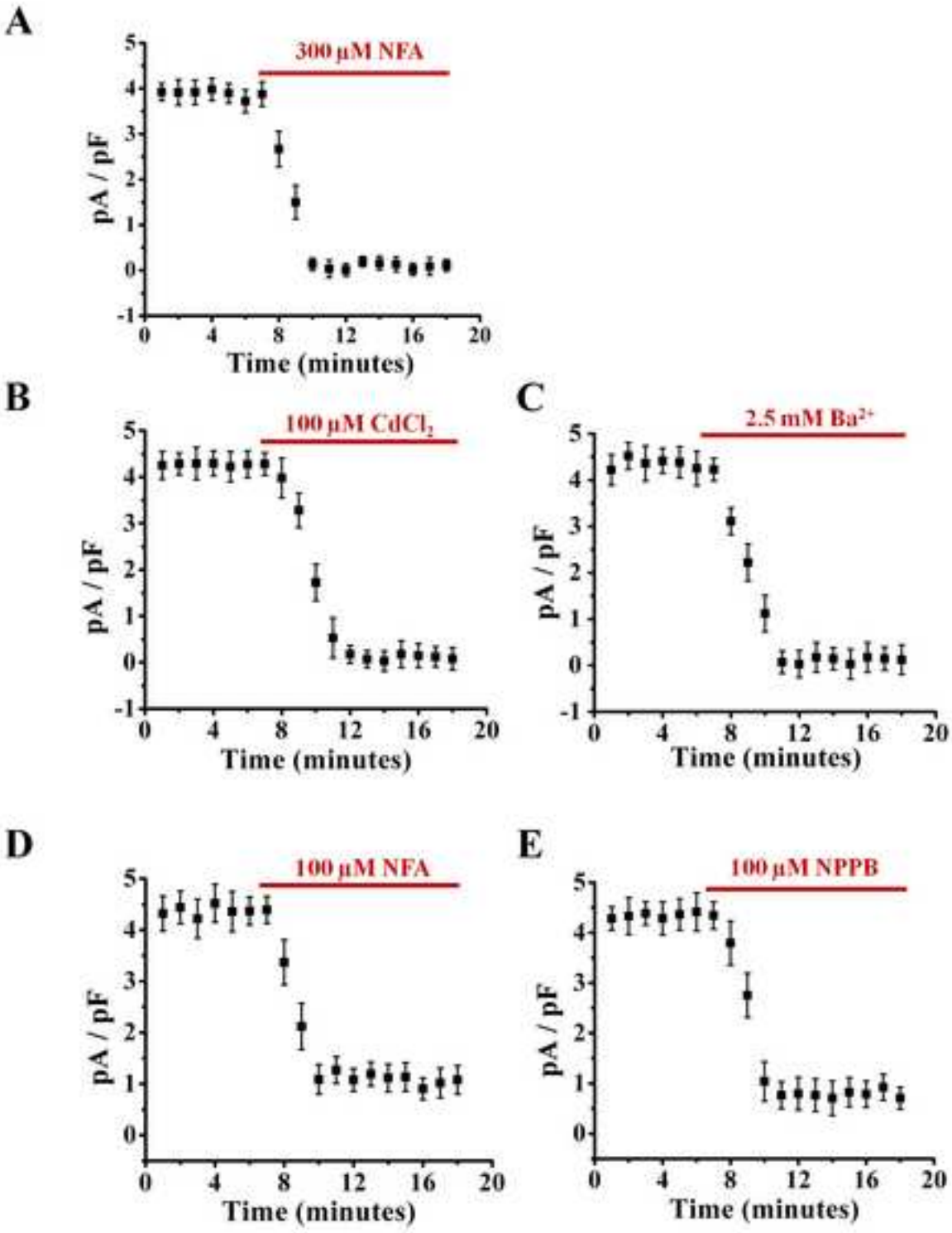

Supplemental Figures 1A-1E

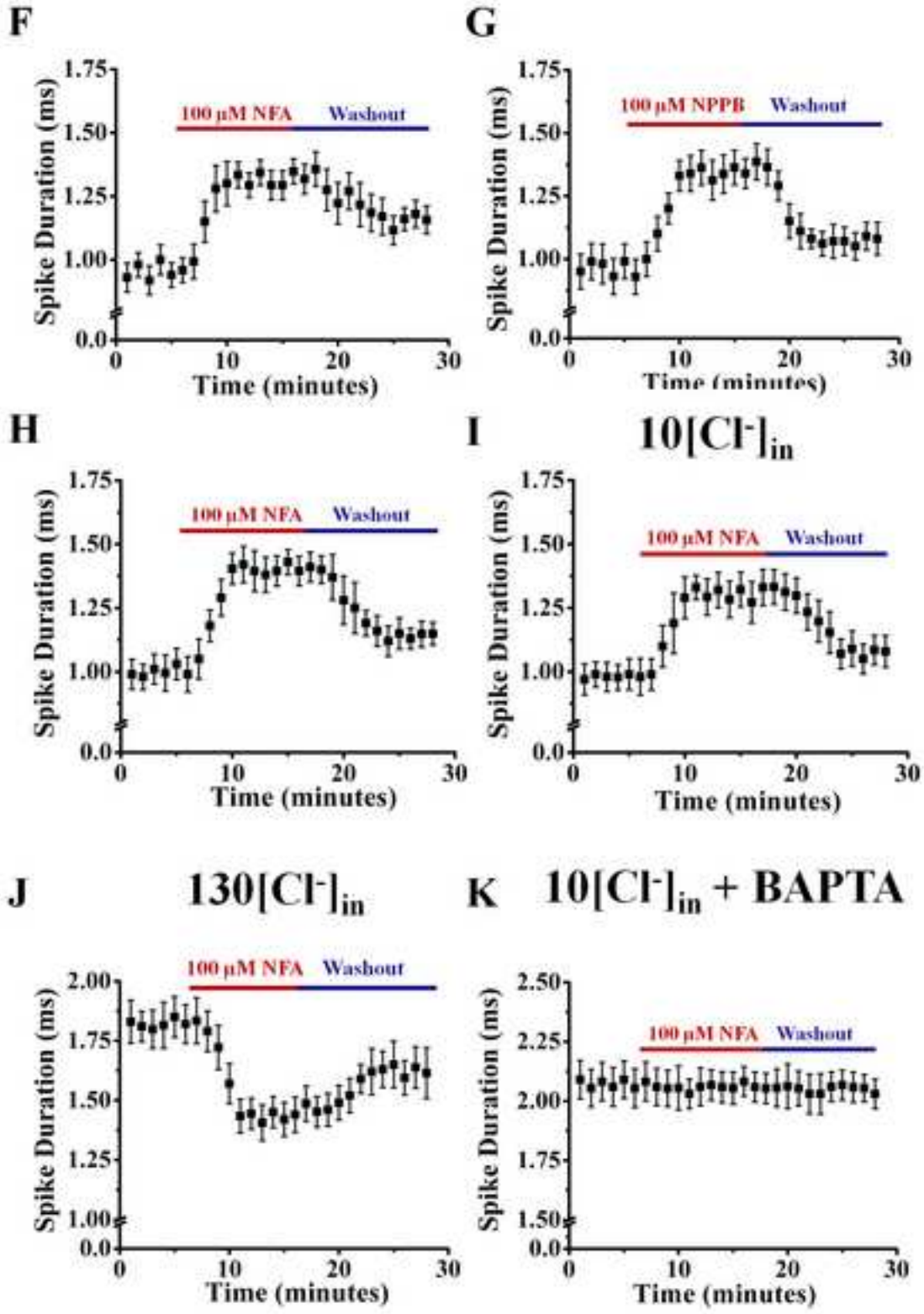

Supplemental Figures 1F-1K

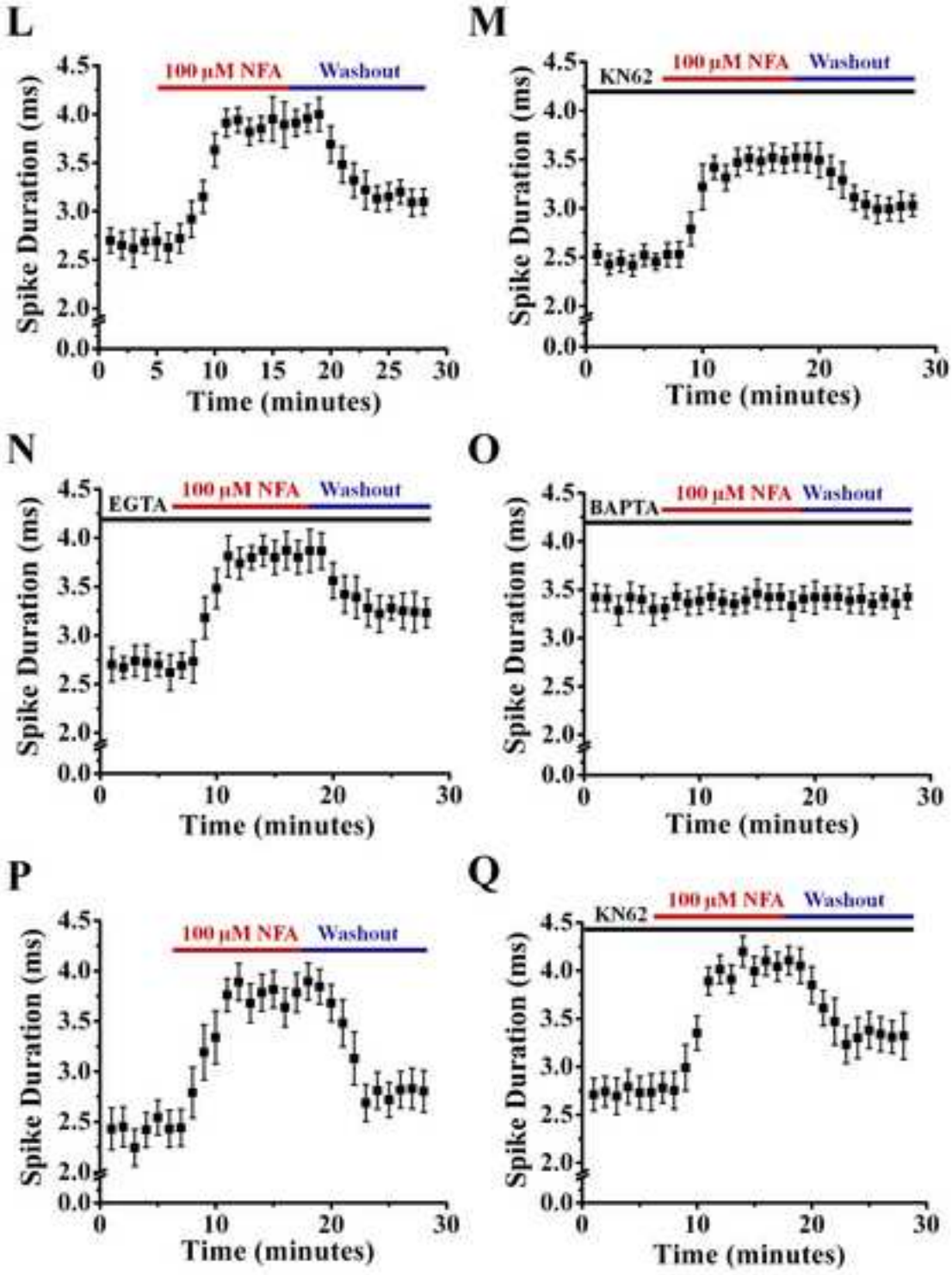

Supplemental Figures 1L-1Q

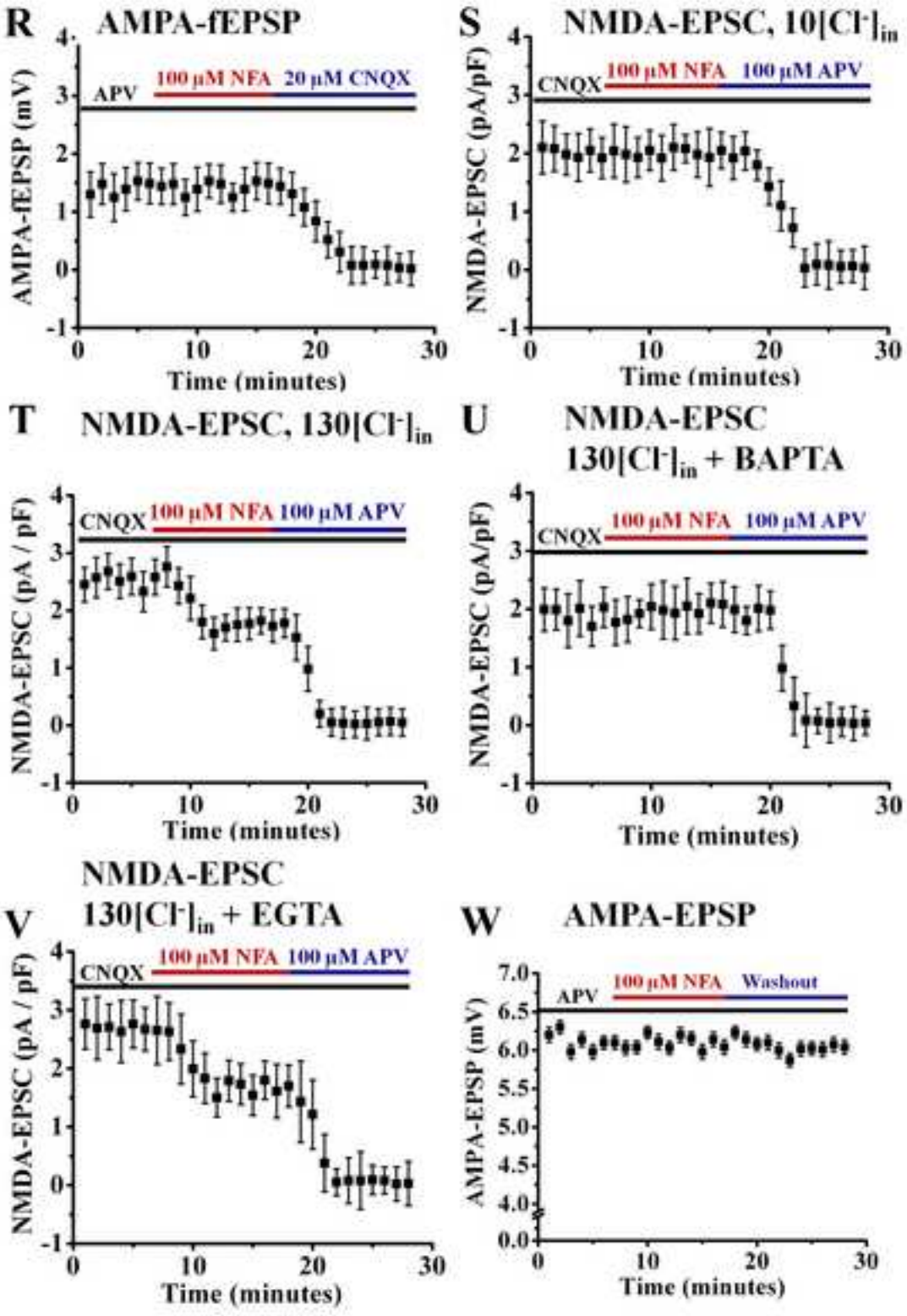

Supplemental Figures 1R-1W

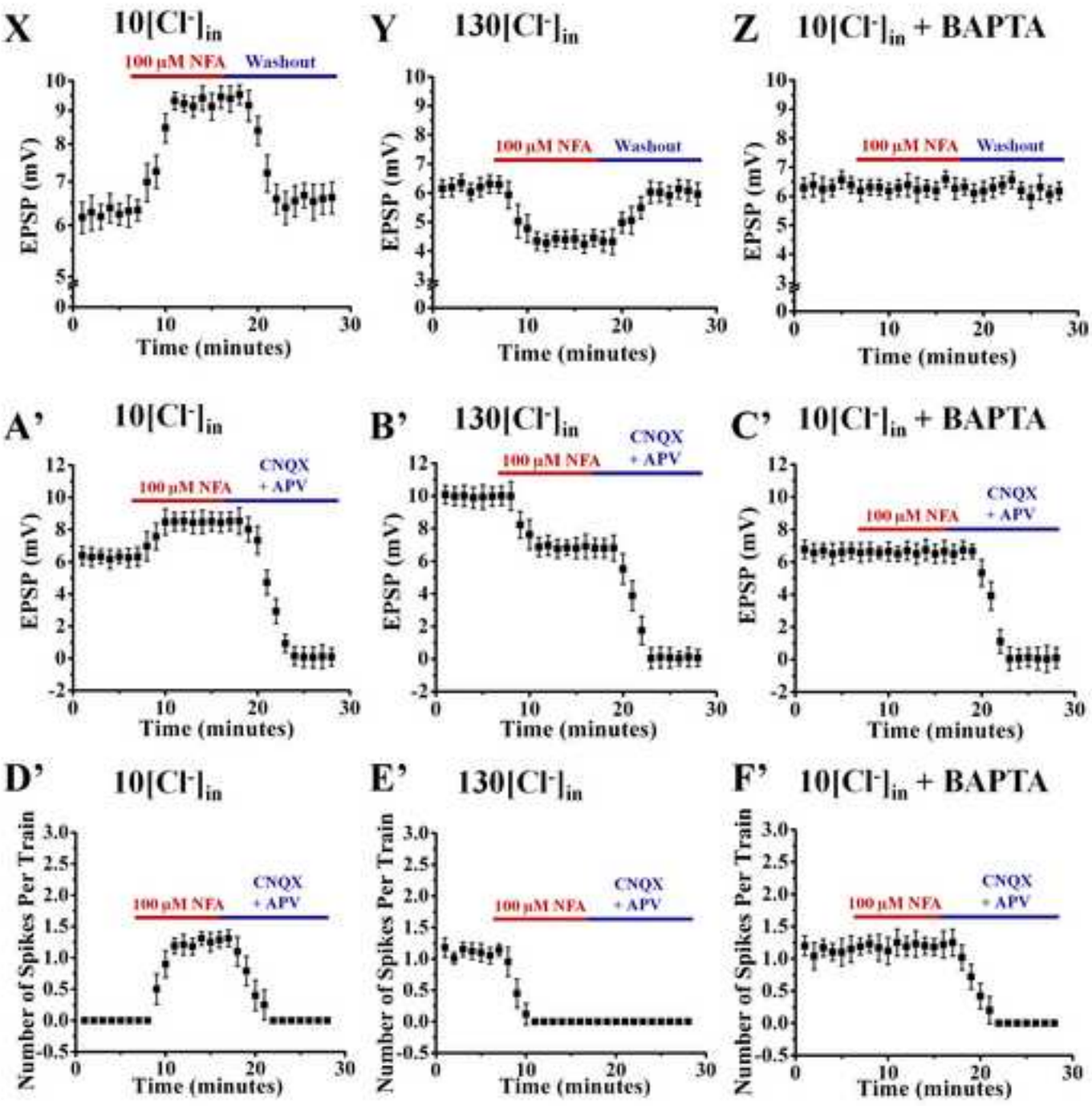

Supplemental Figures 1X-1F'

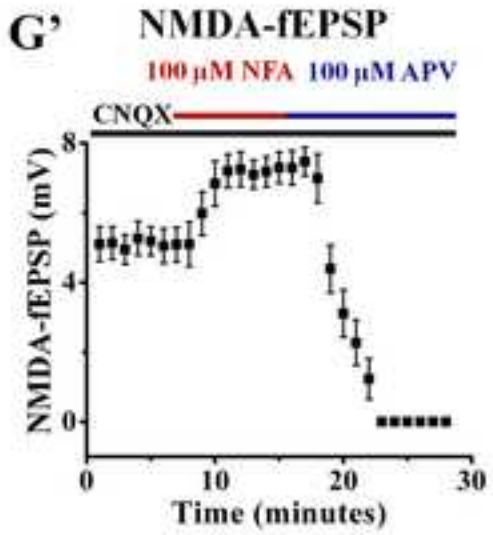

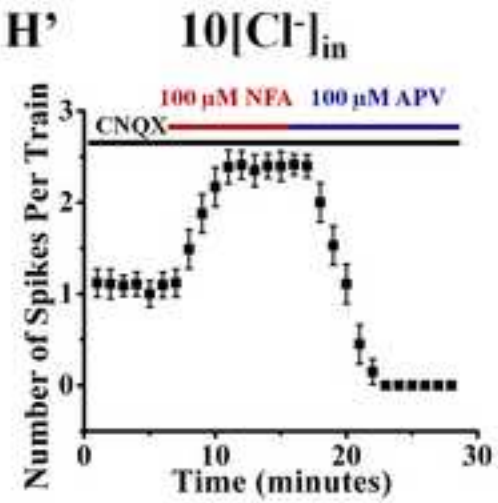

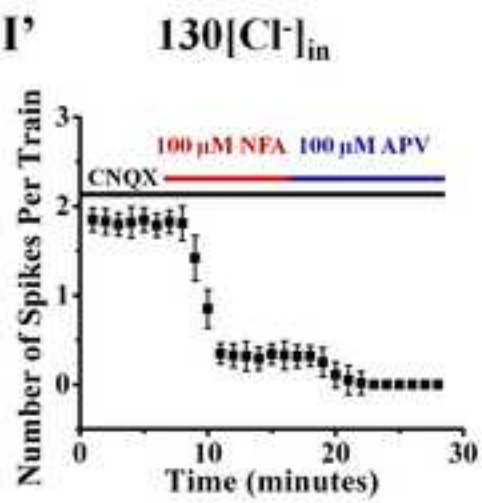

Supplemental Figures 1G'-1I'

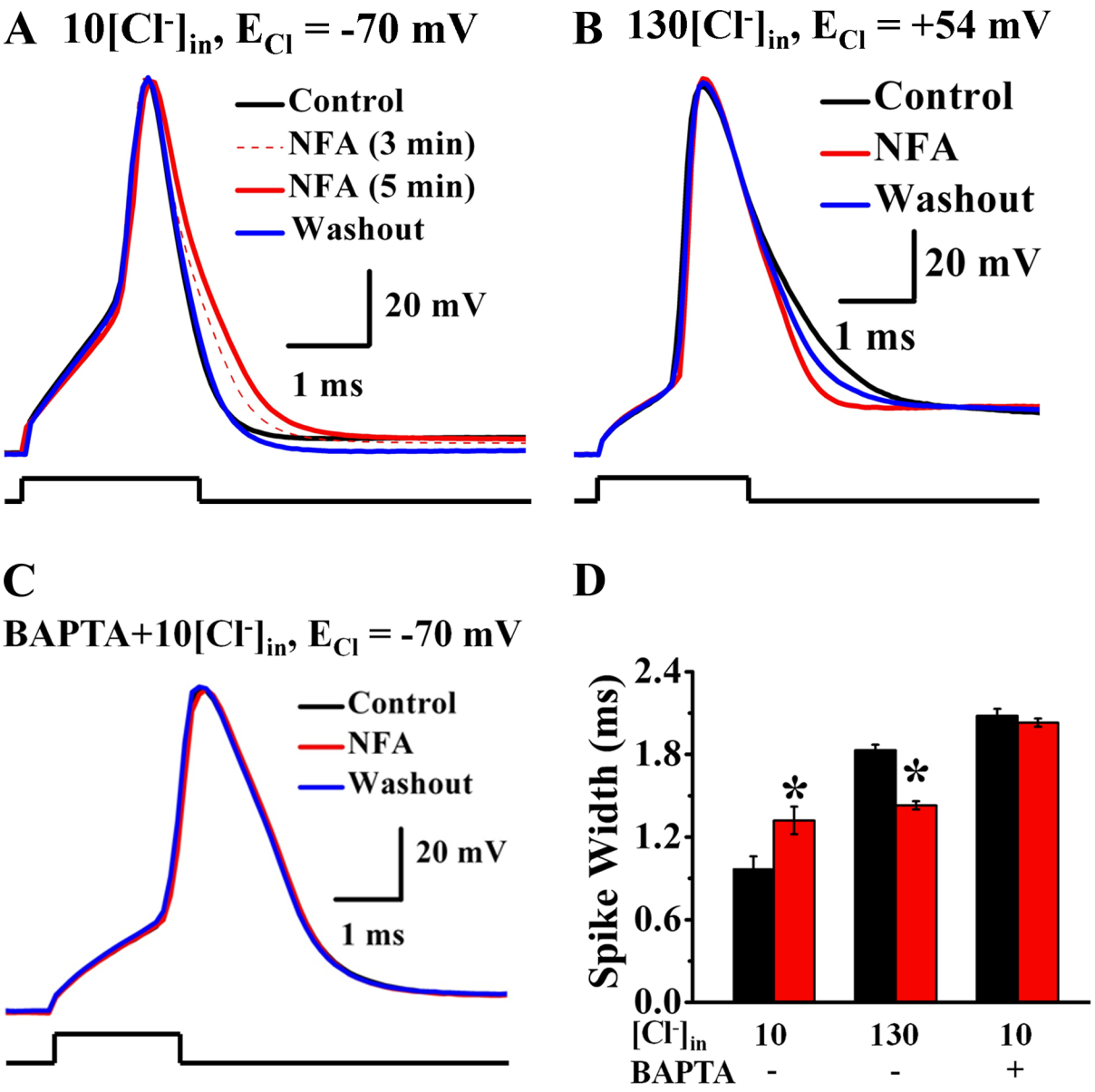

Supplemental Figure 2

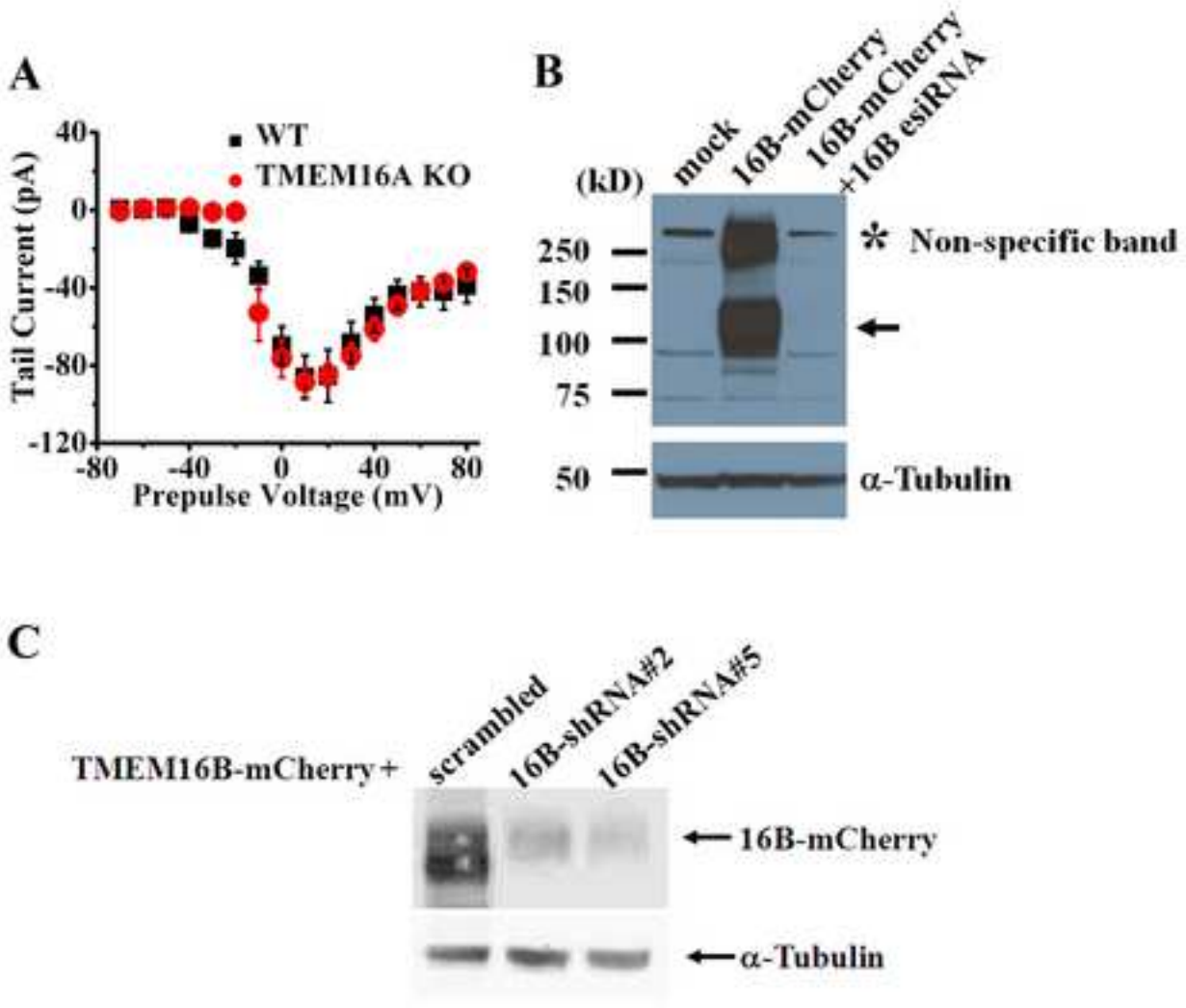

Supplemental Figure 3

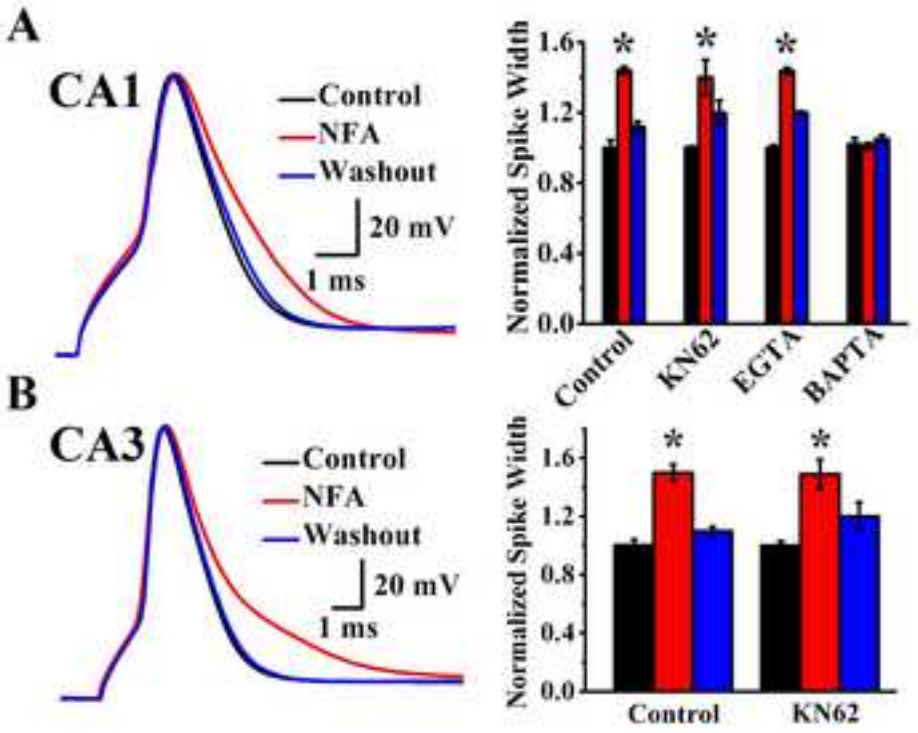

Supplemental Figure 4

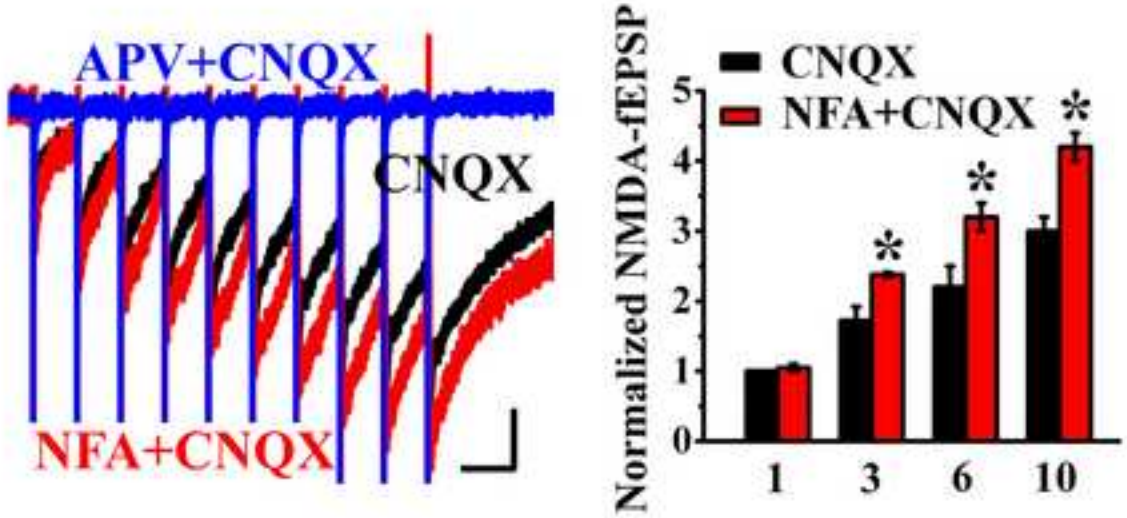

Supplemental Figure 5

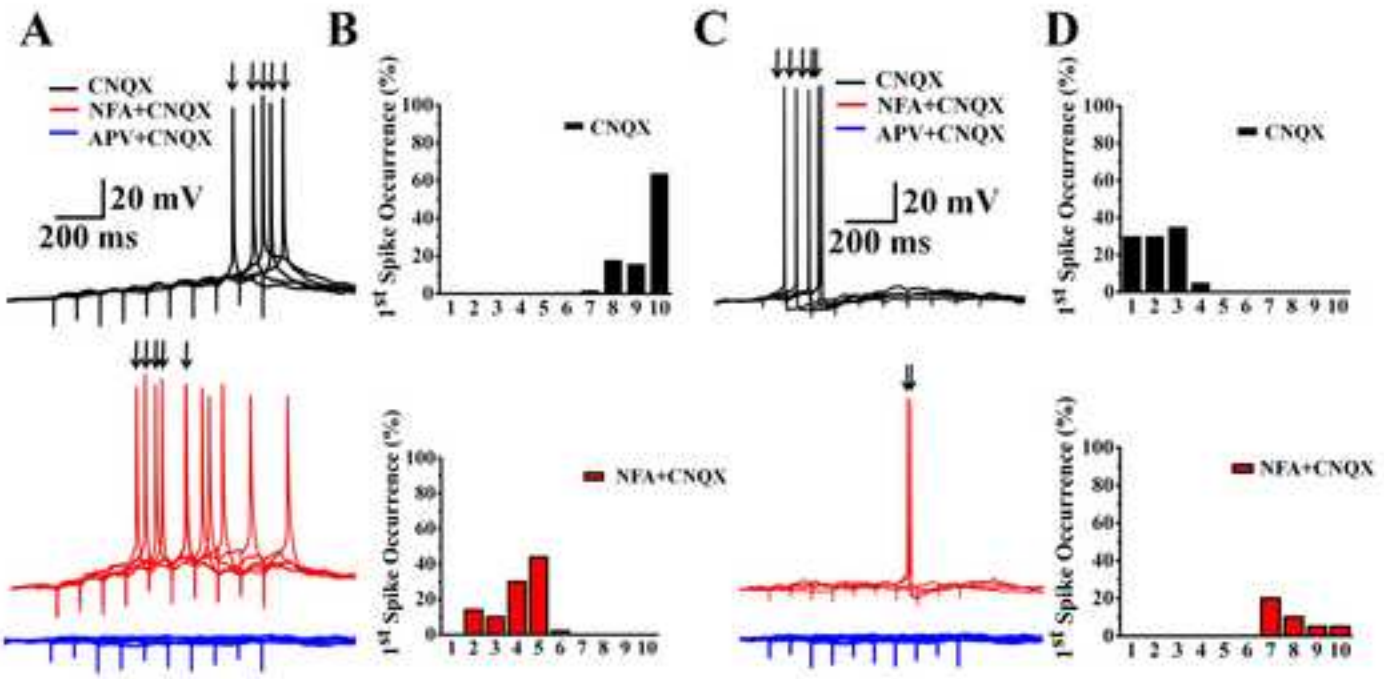

Supplemental Figure 6

SUPPLEMENTAL INFORMATION

SUPPLEMENTAL FIGURE LEGENDS

Supplemental Figure 1. Time course plots for pharmacology experiments.
(A) Summary plot of the current density (pA/pF) of tail current at -65 mV (E_{Cl} = -45 mV) before and after 300 µM NFA (horizontal bar) (n = 25) (Figure 1D).
(B) Summary plot of the current density (pA/pF) of tail current at -90 mV (E_{Cl} = -45 mV) before and after 100 µM $CdCl_2$ (horizontal bar) (n = 10) (Figure 2A).
(C) Summary plot of the current density (pA/pF) of tail current at -90 mV (E_{Cl} = -45 mV) before and after replacing external 2.5 mM Ca^{2+} with 2.5 mM Ba^{2+} (horizontal bar) (n = 13) (Figure 2C).
(D) Summary plot of the current density (pA/pF) of tail current at -90 mV (E_{Cl} = -45 mV) before and after 100 µM NFA (horizontal bar) (n = 9) (Figure 3A).
(E) Summary plot of the current density (pA/pF) of tail current at -90 mV (E_{Cl} = -45 mV) before and after 100 µM NPPB (horizontal bar) (n = 10) (Figure 3A).
(F) Summary plot of CA1 action potential duration (measured at 1/3 total spike height, acute slices, 35°C) before and after 100 µM NFA (red horizontal bar) and during washout (blue horizontal bar) (n = 9) (Figure 3B). For the spike elicited by 2 ms current injection, NFA does not significantly change the mean threshold (-37.4 ± 1.79 mV and -36.7 ± 1.32 mV before and after NFA, respectively, n = 9, $p > 0.05$) or the mean spike amplitude measured from the resting membrane potential (115 ± 5.31 mV and 114.18 ± 6.12 mV before and after NFA, respectively, n = 9, $p > 0.05$) (also see Table 1).
(G) Summary plot of CA1 action potential duration (measured at 1/3 total spike height, acute slices, 35°C) before and after 100 µM NPPB (red horizontal bar) and during washout (blue horizontal bar) (n = 9) (Figure 3C). For the single action potential elicited by 2 ms current injection, NPPB does not significantly change the mean thresholds (-36.7 ± 1.65 mV and -35.8 ± 1.49 mV before and after NPPB, respectively, n = 9, $p > 0.05$) or the mean spike amplitudes (116 ± 4.38 mV and 117 ± 5.16 mV before and after NPPB, respectively, n = 9, $p > 0.05$).
(H) Summary plot of the CA3 action potential duration (measured at 1/3 total spike height, acute slices, 35°C) before and after 100 µM NFA (red horizontal bar) and during washout (blue horizontal bar) (n = 10) (Figures 5A and 5B). Blocking CaCC did not alter mean spike threshold (before and after NFA: -34.7 ± 2.18 mV and -35.7 ± 2.65 mV respectively, n = 10, $p > 0.05$) or mean spike amplitude (before and after NFA: 113.2 ± 4.23 mV and 115.2 ± 3.83 mV, n = 10, $p > 0.05$).
(I) Summary plot of the CA1 action potential duration (10 mM $[Cl^-]_{in}$, measured at 1/3 total spike height, acute slices, 35°C) before and after 100 µM NFA (red horizontal bar) and during washout (blue horizontal bar) (n = 6) (Supplemental Figure 2A).
(J) Summary plot of the CA1 action potential duration (130 mM $[Cl^-]_{in}$, measured at 1/3 total spike height, acute slices, 35°C) before and after 100 µM NFA (red horizontal bar) and during washout (blue horizontal bar) (n = 6) (Supplemental Figure 2B).
(K) Summary plot of the CA1 action potential duration (10 mM $[Cl^-]_{in}$ + 10 mM BAPTA, measured at 1/3 total spike height, acute slices, 35°C) before and after 100 µM NFA (red horizontal bar) and during washout (blue horizontal bar) (n = 5) (Supplemental Figure 2C).
(L) Summary plot of the CA1 action potential duration (10 mM $[Cl^-]_{in}$, measured at 1/3 total spike height, acute slices, room temperature) before and after 100 µM NFA (red horizontal bar) and

during washout (blue horizontal bar) (n = 10) (Supplemental Figure 4A, leftmost set of bars for "Control").
(M) Summary plot of the CA1 action potential duration in the presence of 100 µM KN62 (10 mM $[Cl^-]_{in}$, measured at 1/3 total spike height, acute slices, room temperature) before and after 100 µM NFA (red horizontal bar) and during washout (blue horizontal bar) (n = 9) (Supplemental Figure 4A, second leftmost set of bars for "KN62").
(N) Summary plot of the CA1 action potential duration in the presence of 10 mM EGTA (10 mM $[Cl^-]_{in}$, measured at 1/3 total spike height, acute slices, room temperature) before and after 100 µM NFA (red horizontal bar) and during washout (blue horizontal bar) (n = 5) (Supplemental Figure 4A, second rightmost set of bars for "EGTA").
(O) Summary plot of the CA1 action potential duration in the presence of 10 mM BAPTA (10 mM $[Cl^-]_{in}$, measured at 1/3 total spike height, acute slices, room temperature) before and after 100 µM NFA (red horizontal bar) and during washout (blue horizontal bar) (n = 5) (Supplemental Figure 4A, rightmost set of bars for "BAPTA").
(P) Summary plot of the CA3 action potential duration (10 mM $[Cl^-]_{in}$, measured at 1/3 total spike height, acute slices, room temperature) before and after 100 µM NFA (red horizontal bar) and during washout (blue horizontal bar) (n = 10) (Supplemental Figure 4B, left set of bars for "Control").
(Q) Summary plot of the CA3 action potential duration in the presence of 100 µM KN62 (10 mM $[Cl^-]_{in}$ measured at 1/3 total spike height, acute slices, room temperature) before and after 100 µM NFA (red horizontal bar) and during washout (blue horizontal bar) (n = 11) (Supplemental Figure 4B, right set of bars for "KN62").
(R) Summary plot of AMPA-fEPSP (6^{th} response in the train) recorded extracellularly from CA1 in the presence of 100 µM APV (acute slices, 35°C) before and after 100 µM NFA (red horizontal bar) and application of 20 µM CNQX at the end of recording (blue horizontal bar) (n = 7) (Figure 5C).
(S) Summary plot of NMDA-EPSC current density (pA/ pF) in CA1 neurons recorded with 10 mM $[Cl^-]_{in}$ in the presence of 20 µM CNQX (acute slices, 35°C) before and after 100 µM NFA (red horizontal bar) and application of 100 µM APV at the end of recording (blue horizontal bar) (n = 5) (Figure 5D).
(T) Summary plot of NMDA-EPSC current density (pA/ pF) in CA1 neurons recorded with 130 mM $[Cl^-]_{in}$ in the presence of 20 µM CNQX (acute slices, 35°C) before and after 100 µM NFA (red horizontal bar) and application of 100 µM APV at the end of recording (blue horizontal bar) (n = 10) (Figure 5E).
(U) Summary plot of NMDA-EPSC current density (pA/ pF) in CA1 neurons recorded with 130 mM $[Cl^-]_{in}$ and 10 mM BAPTA in the presence of 20 µM CNQX (acute slices, 35°C) before and after 100 µM NFA (red horizontal bar) and application of 100 µM APV at the end of recording (blue horizontal bar) (n = 10) (Figure 5F).
(V) Summary plot of NMDA-EPSC current density (pA/ pF) in CA1 neurons recorded with 130 mM $[Cl^-]_{in}$ and 10 mM EGTA in the presence of 20 µM CNQX (acute slices, 35°C) before and after 100 µM NFA (red horizontal bar) and application of 100 µM APV at the end of recording (blue horizontal bar) (n = 10) (Figure 5G).
(W) Summary plot of AMPA-EPSP amplitude (mV) in CA1 neurons with 10 mM $[Cl^-]_{in}$ in the presence of 100 µM APV (acute slices, 35°C) before and after 100 µM NFA (red horizontal bar) and washout (blue horizontal bar) (n = 11) (Figure 5I and 5J).
(X) Summary plot of EPSP amplitude (mV) in CA1 neurons with 10 mM $[Cl^-]_{in}$ (acute slices,

35°C) before and after 100 μM NFA (red horizontal bar) and washout (blue horizontal bar) (n = 10) (Figure 6A and 6B, left).
(Y) Summary plot of EPSP amplitude (mV) in CA1 neurons with 130 mM $[Cl^-]_{in}$ (acute slices, 35°C) before and after 100 μM NFA (red horizontal bar) and washout (blue horizontal bar) (n = 9) (Figure 6B, middle).
(Z) Summary plot of EPSP amplitude (mV) in CA1 neurons with 10 mM $[Cl^-]_{in}$ + 10 mM BAPTA (acute slices, 35°C) before and after 100 μM NFA (red horizontal bar) and washout (blue horizontal bar) (n = 16) (Figure 6B, right).
(A') Summary plot of summated EPSP amplitude (mV) (the third EPSP) in CA1 neurons with 10 mM $[Cl^-]_{in}$ (acute slices, 35°C) before and after 100 μM NFA (red horizontal bar) and 20 μM CNQX + 100 μM APV at the end of recording (blue horizontal bar) (n = 8) (Figure 6C and 6D, left).
(B') Summary plot of summated EPSP amplitude (mV) (the third EPSP) in CA1 neurons with 130 mM $[Cl^-]_{in}$ (acute slices, 35°C) before and after 100 μM NFA (red horizontal bar) and 20 μM CNQX + 100 μM APV at the end of recording (blue horizontal bar) (n = 9) (Figure 6D, middle).
(C') Summary plot of summated EPSP amplitude (mV) (the third EPSP) in CA1 neurons with 10 mM $[Cl^-]_{in}$ + 10 mM BAPTA (acute slices, 35°C) before and after 100 μM NFA (red horizontal bar) and 20 μM CNQX + 100 μM APV at the end of recording (blue horizontal bar) (n = 5) (Figure 6D, right).
(D') Summary plot of average number of spikes in CA1 neurons per train of 5 stimuli with 10 mM $[Cl^-]_{in}$ (acute slices, 35°C) before and after 100 μM NFA (red horizontal bar) and 20 μM CNQX + 100 μM APV at the end of recording (blue horizontal bar) (n = 7) (Figure 6E and 6F, left).
(E') Summary plot of average number of spikes in CA1 neurons per train of 5 stimuli with 130 mM $[Cl^-]_{in}$ (acute slices, 35°C) before and after 100 μM NFA (red horizontal bar) and 20 μM CNQX + 100 μM APV at the end of recording (blue horizontal bar) (n = 8) (Figure 6F, middle).
(F') Summary plot of average number of spikes in CA1 neurons per train of 5 stimuli with 10 mM $[Cl^-]_{in}$ + 10 mM BAPTA (acute slices, 35°C) before and after 100 μM NFA (red horizontal bar) and 20 μM CNQX + 100 μM APV at the end of recording (blue horizontal bar) (n = 5) (Figure 6F, right).
(G') Summary plot of NMDA-fEPSP (6^{th} response in the train) recorded extracellularly from CA1 in the presence of 20 μM CNQX (acute slices, room temperature) before and after 100 μM NFA (red horizontal bar) and application of 100 μM APV at the end of recording (blue horizontal bar) (n = 8) (Supplemental Figure 5).
(H') Summary plot of average number of spikes in CA1 neurons per train of 10 stimuli with 10 mM $[Cl^-]_{in}$ in the presence of 20 μM CNQX (acute slices, room temperature) before and after 100 μM NFA (red horizontal bar) and 100 μM APV at the end of recording (blue horizontal bar) (n = 10) (Supplemental Figures 6A and 6B).
(I') Summary plot of average number of spikes in CA1 neurons per train of 10 stimuli with 130 mM $[Cl^-]_{in}$ in the presence of 20 μMCNQX (acute slices, room temperature) before and after 100 μM NFA (red horizontal bar) and 100 μM APV at the end of recording (blue horizontal bar) (n = 10) (Supplemental Figures 6C and 6D).

Supplemental Figure 2. Blocking CaCC modulates action potential duration in opposite ways with opposite Cl^- gradients, while internal BAPTA eliminates CaCC modulation of action potential duration (acute slices, 35 ^oC).

(A) At 35°C, reducing CaCC in acute hippocampal slices with 100 µM NFA (red dotted line, 3 min after adding NFA; red solid line, 5 min after NFA addition) slows the action potential repolarization (1.32 ± 0.10 ms) compared to action potentials prior to NFA application (control, black, 0.97 ± 0.09 ms, n = 6, $p < 0.001$) and after washout of NFA (blue). Recording were performed with 10 $[Cl^-]_{in}$ (E_{Cl} = -64.4 mV) under physiological condition. Resting membrane voltage is between -65 to -70 mV and NFA did not significantly alter spike threshold (before NFA, -37.4 ± 1.79 mV vs. after NFA, -36.7 ± 1.32 mV, n =9, $p > 0.05$) or spike amplitude (before NFA, 115 ± 5.31 mV vs. after NFA, 114 ± 6.12 mV, n= 9, $p > 0.05$). See Supplemental Figure 1I for time course plot.

(B) In contrast, in the presence of 130 $[Cl^-]_{in}$ (E_{Cl} = +54 mV) at 35°C, reducing CaCC with 100 µM NFA (red, 1.43 ± 0.03 ms) speeds up the action potential repolarization (black, control, 1.83 ± 0.04 ms, n = 6, $p < 0.001$). Resting membrane voltage is between -65 to -70 mV and NFA did not significantly alter spike threshold (before NFA, -54.7 ± 1.27 mV vs. after NFA, -53.9 ± 1.59 mV, n = 12, $p > 0.05$) or spike amplitude (before NFA, 113 ± 4.11 mV vs. after NFA, 114 ± 3.77 mV, n = 12, $p > 0.05$). See Supplemental Figure 1J for time course plot.

(C) At 35°C, NFA has no effect on action potential duration when 10 mM BAPTA was included with 10 mM $[Cl^-]_{in}$(2.08 ± 0.05 ms vs. 2.03 ± 0.03 ms, n = 5, $p > 0.05$). Resting membrane voltage is between -65 to -70 mV and NFA did not significantly alter spike threshold (before NFA, -36.2 ± 1.67 mV vs. after NFA, -35.2 ± 1.73 mV, n = 8, $p > 0.05$) or spike amplitude (before NFA, 114 ± 3.85 mV vs. after NFA 114 ± 4.15 mV, n= 8, $p > 0.05$). See Supplemental Figure 1K for time course plot.

(D) Summary of the opposing effect of NFA on spike duration between low and high internal Cl^- and the lack of effect when BAPTA was included to chelate internal calcium (see Table 1).

Supplemental Figure 3. Control experiments show that TMEM16A is not responsible for hippocampal CaCC and the antibodies against TMEM16B are specific.

(A) Ca^{2+}-activated Cl^- current is still present in hippocampal slices from TMEM16A knockout mice (wildtype, n = 7, TMEM16A knockout, n = 11, p = 0.9). Recordings were performed at room temperature.

(B) Rabbit polyclonal antibody against TMEM16B recognized the exogenously expressed TMEM16B-mCherry in HEK293 cells (middle lane). Co-transfection of TMEM16B-mCherry with TMEM16B esiRNA to knock down TMEM16B expression (right lane) dramatically reduced the expression of TMEM16B-mCherry in HEK293 cells two days after transfection. Arrow points to 132 kD, the molecular weight of TMEM16B-mCherry. The heavier band of about twice the molecular weight in the middle lane is possibly a dimer of TMEM16B-mCherry. * indicates non-specific signal due to antibody cross reactivity. Bottom panel is the α-tubulin loading control.

(C) Knock down of the exogenously expressed TMEM16B by shRNA. HEK293 cells were co-transfected with plasmids expressing mouse TMEM16B-mCherry and a scrambled shRNA, 16B-shRNA #2, or 16B-shRNA #5. Total proteins were extracted two days after transfection and subjected to western blotting with anti-DsRed antibody. In this representative western blot, 16B-shRNA #2 and 16B-shRNA #5 decreased the protein level of TMEM16B-mCherry by 81% and 87%, respectively, compared to the scrambled shRNA control. α-tubulin was probed for as a loading control.

Supplemental Figure 4. Hippocampal CaCC is activated by Ca^{2+}, not CaMKII (acute slices, room temperature).
(A) Increase of action potential width by CaCC blocker (100 μM NFA) is observed in CA1 pyramidal neurons in acute slices (P14-21) (left, control, black, 2.70 ± 0.01 ms; NFA, red, 3.91 ± 0.02 ms; n = 10, $p < 0.05$). The broadening effect is still observed in the presence of 100 μM CaMKII blocker, KN62, suggesting that CaCC is activated by Ca^{2+}, but not CaMKII (right, KN62; control, black, 2.53 ± 0.02 ms; NFA, red, 3.52 ± 0.03 ms; n = 9, $p < 0.005$). The broadening effect persists in the presence of 10 mM EGTA, suggesting that CaCCs and voltage-gated Ca^{2+} channels are in close proximity so that the slower Ca^{2+} chelator EGTA fails to prevent calcium influx through calcium channels to activate CaCCs (right, EGTA; control, black, 2.71 ± 0.04 ms; NFA, red, 3.88 ± 0.04 ms, n = 5, $p < 0.001$). In contrast, when 10 mM BAPTA was included in the patch pipette to chelate internal Ca^{2+}, NFA had no effect, suggesting that the faster Ca^{2+} chelator BAPTA prevented calcium influx through calcium channels from activating CaCC (right, BAPTA; control, black, 3.42 ± 0.13 ms, NFA, red, 3.41 ± 0.17 ms; n = 5, $p = 0.9$). Blue indicates washout. Recordings were performed in acute slices at room temperature in all panels in this figure. Resting membrane voltage is between -65 to -70 mV and NFA did not significantly alter spike threshold or spike amplitude in control solution: spike threshold, -35.4 ± 1.85 mV vs. -34.5 ± 1.32 mV; spike amplitude, 115 ± 3.56 mV vs. 115 ± 4.21 mV (n = 10, $p > 0.05$); in the presence of KN62: spike threshold, -34.7 ± 1.81 vs. -35.9 ± 1.23 mV; spike amplitude, 113 ± 4.59 mV vs. 114 ± 4.84 mV (n = 9, $p > 0.05$); with intracellular EGTA: spike threshold, -36.5 ± 2.28 mV vs. -36.1 ± 1.92 mV; spike amplitude, 114 ± 3.96 mV vs. 114 ± 4.95 mV (n = 5, $p > 0.05$); or with intracellular BAPTA: spike threshold, -36.8 ± 3.28 mV vs. -36.5 ± 4.21 mV, spike amplitude, 115 ± 3.44 mV vs. 114 ± 5.13 mV (n =5, $p > 0.05$). See Supplemental Figure 1L-O for time course plots.
(B) 100 μM NFA increases the duration of action potential in CA3 pyramidal neurons in acute slices (P14-21), as evident from superimposed traces on the left and the bar graph on the right, in the absence of 100 μM KN62 (right, control, black, 2.43 ± 0.09 ms; NFA, red, 3.86 ± 0.13 ms) (n = 10, $p < 0.005$) and in the presence of the CaMKII inhibitor (right, KN62; control, black, 2.75 ± 0.024 ms; NFA, red, 4.12 ± 0.04 ms; n = 11, $p < 0.005$). Blue indicates washout. Recordings were performed at room temperature. Resting membrane voltage is between -65 to -70 mV and NFA did not significantly alter spike threshold or spike amplitude in control solution: spike threshold, -35.8 ± 2.81 mV vs. -37.6 ± 3.33 mV; spike amplitude, 114 ± 3.77 mV vs. 112 ± 3.31 mV; or in the presence of KN62: spike threshold, -34.4 ± 4.12 mV vs. -35.6 ± 3.75mV; spike amplitude, 113 ± 4.32 mV vs. 114 ± 3.95 mV (n = 11, $p > 0.05$). See Supplemental Figure 1P and 1Q for time course plots.

Supplemental Figure 5. CaCC shows activity-dependent modulation of NMDA receptor- mediated synaptic responses monitored with extracellular field recording from hippocampal slices bathed in 20 μM CNQX.
Left, 100 μM NFA has progressively stronger effect on NMDA-fEPSP recorded in CA1 dendritic field by delivering a train of 10 stimuli at 10 Hz to Schaffer collateral axons. Scale bar: 100 ms, 1 mV. Right, bar graphs of the field recordings showing that NFA increases the 3^{rd}, 6^{th}, and 10^{th} (n = 8, $p < 0.01$) but not the 1^{st} NMDA-fEPSP amplitude (n = 8, $p = 0.8$). Black, control (in the presence of 20 μM CNQX); red, 100 μM NFA plus 20 μM CNQX; blue, 100 μM APV plus 20 μM

CNQX applied at the end of the experiment. Recordings obtained from acute slices at room temperature. See Supplemental Figure 1G' for time course plot.

Supplemental Figure 6. CaCC modulates NMDA receptor-mediated synaptic responses in opposite ways when Cl^- gradient is inverted.
(A) When CaCC is inhibitory with 10 mM $[Cl^-]_{in}$ (E_{Cl} = -64.4 mV), CaCC blocker NFA (100 μM) enhances NMDA-EPSP spike coupling (red) compared to control (black) (20 μM CNQX present throughout the experiment). Blue, 100 μM APV applied at the end of the experiment. Shown are 5 superimposed sweeps with each of the 5 arrows indicating first spike in each recording of responses to 10 nerve stimuli at 10 Hz. Recordings performed in acute slices at room temperature for all panels of this figure.
(B) CaCC is inhibitory with 10 mM $[Cl^-]_{in}$ (E_{Cl} = -64.4 mV), CaCC blocker NFA (red) (100 μM) shortens the latency to first spike and increases the average number of spikes per train recorded from hippocampal slices (in the presence of 20 μM CNQX). Histogram quantifies the occurrence of the first spike in the responses to 10 stimuli at 10 Hz. Average latency (in seconds): control 1.14 ± 0.01, NFA 0.57 ± 0.02 (n = 10, $p < 0.001$). Average number of spikes per train: control 1.12 ± 0.05, NFA 2.42 ± 0.2 (n = 10, $p < 0.001$). See Supplemental Figure 1H' for time course plot.
(C) When CaCC is excitatory with 130 mM $[Cl^-]_{in}$ (E_{Cl} = 0 mV), CaCC blocker NFA (100 μM) reduces NMDA-EPSP spike coupling (red) compared to control (black) (20 μM CNQX present throughout the experiment) (Supplemental 1I'). Blue, 100 μM APV applied at the end of the experiment. Shown are 5 superimposed sweeps with each of the 5 arrows indicating first spike in each recording of responses to 10 nerve stimuli at 10 Hz.
(D) When CaCC is excitatory with 130 mM $[Cl^-]_{in}$ (E_{Cl} = 0 mV), CaCC blocker NFA (red) (100 μM) increases the latency to first spike and decreases the average number of spikes per train recorded from hippocampal slices (in the presence of 20 μM CNQX). Histogram quantifies the occurrence of the first spike in the responses to 10 Hz stimuli. Average latency (in seconds): control, 0.35 ± 0.02, NFA, 0.77 ± 0.09 (n = 10, $p < 0.001$). Average number of spikes per train: control, 1.85 ± 0.22, NFA, 0.35 ± 0.13 (n =10, $p < 0.001$). See Supplemental Figure 1I' for time course plot.

SUPPLEMENTAL EXPERIMENTAL PROCEDURES

in situ Hybridization

A 2.6 kb cDNA fragment complementary to mouse TMEM16B mRNA was subcloned into the pBluescript-SK- plasmid and linearized with BamHI for antisense RNA probe synthesis by T7 transcriptase. The transcribed cRNA was hydrolyzed with sodium carbonate alkaline solution at 60^{o}C for 15 min for better tissue penetration. C57BL/6 mice were deeply anesthetized and then perfused with 4% paraformaldehyde in 0.1 M PBS, pH 7.4. Brains were removed and postfixed overnight in 4% paraformaldehyde/PBS. Brains that were to be sectioned on a cryostat were placed in 30% sucrose in 0.1M PBS (0.1% DEPC treated) until the brains sank and were then embedded in Tissue Tec OCT compound and frozen on dry ice. Frozen brains were sectioned at 20 µm on a cryostat, and sections were mounted on VWR precleaned superfrost plus slides and stored at -80^{o}C. Slides were thawed at room temperature for 5-10 min and were then dried in a 42°C oven for 10 min. Sections were postfixed with 4% paraformaldehyde in 0.1 M PBS for 30 min and then rinsed with 0.5x SSC for 5 min. Sections were treated with Proteinase K (1.25 mg/L) for 30 min, rinsed again with 0.5x SSC for 10 min, and air dried. The sections were covered with 75 µl of prehybridization buffer (2x SSC, 25% formamide, 1% Denhardt's reagent, 10% dextran sulfate, 0.5 mg/ml heparin, 0.5 mg/ml yeast tRNA, and 0.25 mg/ml denatured salmon sperm DNA) and incubated at 42°C for 2 h. After the prehybridization, 0.5 µg of digoxigenin-cRNA probe in 75 µl of hybridization buffer was added to each section. The sections were covered with a baked coverslip and incubated overnight at 55°C in humidified box with 25% formamide/2x SSC. The next day, the coverslips were removed and sections were washed with 2x SSC/10 mM EDTA twice. The sections were treated with RNaseA for 30 min and then washed twice with 2x SSC/EDTA. The stringency wash was 0.5x SSC/10 mM EDTA at 55°C for 2 h. After that, sections were washed with 0.5x SSC. Alkaline phosphatase-conjugated anti-digoxigenin Fab fragment (1:5000) was used to detect the hybridized probes. Nitroblue-tetrazolium-chloride/5-bromo-4-chlor-indolyl-phosphate solution was applied overnight at 4°C to detect the alkaline phosphatase. Sections were then washed with 100mM Tris-HCl (pH 8.5)/1 mM EDTA three times for 10 min each. Then slides were briefly rinsed with water twice and covered with mount medium.

RT-PCR Primers

The following primers specific to mouse TMEM16A, TMEM16B and β-actin were used for PCR amplification of cDNA.

TMEM16A	Forward	5'-GGGCTGACTCCTGAGTACATGG-3'
	Reverse	5'-TCATACATTGGTGTGCTGGGACCC-3'
TMEM16B	Forward	5'-GCATACCCTCTGCACGATGG-3'
	Reverse	5'-GTGACAAAGCCGAACTGAATG-3'
β-actin	Forward	5'-TGATGGTGGGAATGGGTCAGAAG-3'
	Reverse	5'-TCTTTACGGATGTCAACGTCAC-3'

Quantitative RT-PCR

Quantitative PCR (qPCR) was performed using program: incubation at 50ºC for 2 min

and 95ºC for 10 min; followed by 40 cycles of denaturation at 95°C for 15 s, annealing and extension at 60°C for 1min. Dissociation curve of each sample was measured to confirm the specificity of the PCR products. qPCR data were normalized to the internal control GAPDH and analyzed using the ΔΔ CT method. Primers used for qPCR are:

TMEM16B	Forward	5'-ACTTGGAGAGCAAAAGCCAGGGATC-3'
	Reverse	5'-TGGGCTGCAGGGGTGAACTGA-3'
GAPDH	Forward	5'-ACCCAGAAGACTGTGGATGG-3'
	Reverse	5'-ACACATTGGGGGTAGGAACA-3' (Kimura et al., 2005)

Enzymatically Prepared siRNA (esiRNA)

The esiRNAs were prepared as described by Kittler et al (Kittler et al., 2005). A DNA fragment that corresponds to 1529-1951 of the mouse *TMEM16B* mRNA (NCBI accession NM_153589.2) was amplified by PCR with primers containing the T7 polymerase promoter sequence. The PCR product was used as the template to make double-stranded RNA (dsRNA) by in vitro transcription (MEGAscript® T7 Kit, Ambion) and slow annealing. The dsRNA was purified with the MEGAclear Kit (Ambion). Ten mg of dsRNA was digested in a 100 mL reaction by ShortCut RNase III (NEB) to generate a pool of short esiRNA with an average size of 21 nucleotides. The esiRNAs were purified with the RNeasy Mini Kit (Qiagen). Primers used to prepare the template for in vitro transcription are:
Forward: 5'- GCTAATACGACTCACTATAGGGAGAGATGTGTCCCCTGTGTGACAA -3'
Reverse: 5'- GCTAATACGACTCACTATAGGGAGAGGAGAACGTCAGGGCAATCAT -3'

Transfection and Western Blotting

HEK293 cells were transfected using Lipofectamine^{TM} 2ooo (Invitrogen) with a plasmid expressing mouse TMEM16B-mCherry with or without co-transfection of shRNAs or 10 nM TMEM16B esiRNA. Cells were harvested 2 days after transfection. Preparation of whole cell lysates and western blotting were performed as described in Experimental Procedures.

Electrophysiology

Hippocampal Culture Recording

For tail current recordings in hippocampal cultured neurons, the pipettes were filled with the following (mM): 23 mM internal Cl^- solution: 10 HEPES, 0.2 EGTA, 125 Cs-gluconate, 18 CsCl, 5 TEACl. 10 mM internal Cl^- solution: 10 HEPES, 0.2 EGTA, 138 Cs-gluconate, 5 CsCl, 5 TEACl. 5 mM internal Cl^- solution: 10 HEPES, 0.2 EGTA, 143 Cs-gluconate, 5 TEACl. pH = 7.2-7.4, adjusted with CsOH, ~300 mosm.

Internal solution containing BAPTA for tail current recording (mM): 10 BAPTA, 10 HEPES, 0.2 EGTA, 125 Cs-gluconate, 18 CsCl, 5 TEACl, pH 7.2-7.4, ~ 300 mosm. The external bath solution for tail current recordings contained (mM unless specified) (mM): 140 NMDG-Cl, 20 HEPES, 1.3 $MgCl_2$, 2.5 $CaCl_2$, 5 4-AP, 1 µM TTX, 50 µM PTX.

A 200 ms depolarization prepulse from -70 mV holding potential to 0 mV was used to elicit inward Ca^{2+} current followed by a long tail current (100s of ms before returning to baseline). For obtaining current-voltage relationship for the tail current, tail current obtained without the depolarization prepulse was subtracted from the tail current obtained with the depolarization prepulse to rid of background current. Voltage steps from -100 to -30 mV (delta 5 mV or 10 mV) were placed on the tail current region, and the

subtracted tail current was plotted as function of the voltage. Reversal potential was the voltage at which the subtracted tail current changed directions. In the $CdCl_2$ experiment 100 μM $CdCl_2$ was added to block Ca^{2+} current hence eliminating Ca^{2+}- activated Cl^- tail current. $CaCl_2$ was replaced with $BaCl_2$ during the Ba^{2+} replacement experiment. 10 mM BAPTA was added to the internal solution to chelate internal Ca^{2+} thus preventing Ca^{2+}-activated Cl^- current activation in the BAPTA experiment. For dose response curves of NFA and NPPB block on tail current, 0.1, 0.3, 1, 10, 30, 100, 300, 1000 μM were used. Only recordings with access resistance < 10 MΩ and with access resistance changing < 10% were kept. 60-90% compensation was applied.

To record CaCC by raising intracellular free Ca^{2+}, the following solutions were used (pH 7.2-7.4, ~ 300 mosm): external, 136 mM TEACl, 2 mM $MgCl_2$, 20 mM HEPES, 20 mM glucose, 300 nM TTX, 5 mM 4-AP, 100μM $CdCl_2$, 20μM KYN, 50 μM PTX; internal, 129 mM TEACl, 2 mM $MgCl_2$, 20 mM HEPES, 5 mM EGTA, 3.8 mM $CaCl_2$ (0.5 μM Ca^{2+}, calculated at www.stanford.edu/~cpatton/maxc.html). Voltage steps from -80 to +80 mV (10 mV intervals) were applied from holding potential of 0 mV (E_{Cl} ~ 0) both without free intracellular Ca^{2+} and with 0.5 μM intracellular Ca^{2+}, and the current recorded in the presence of 300 μM NFA was subtracted from that recorded prior to NFA application.

Acute Hippocampal Slice Recording

To record action potentials in acute slices, 35ºC whole cell recordings (current- clamp mode) from CA1 and CA3 pyramidal neurons were obtained with the following internal solution (mM): 140 K-gluconate, 10 KCl, 10 HEPES, 0.2 EGTA, 4 Mg-ATP, 0.4 Na-GTP, pH 7.2-7.4, adjusted with KOH, ~ 300 mosm. ACSF was used as the external solution (including 50 μM PTX for all recordings and additional 100 μM KN62 for the CaMKII experiment). 2 ms current injection (just suprathreshold) was used to elicit a single action potential. For control experiments with inverted Cl^- gradient (E_{Cl} is +54 mV instead of -64.4 mV as with physiological 10 mM $[Cl^-]_{in}$), internal solution contained 130 mM $[Cl^-]_{in}$ solution (mM): 10 K-gluconate, 130 KCl, 10 HEPES, 0.2 EGTA, 4 MgATP, 0.4 Na_3GTP, pH 7.2-7.4, adjusted with KOH, ~ 300 mosm; external solution contained oxygenated (95% O_2-5% CO_2) 15.1 mM $[Cl^-]_{out}$ ACSF: 114 Na-gluconate, 5 NaCl, 2.5 KCl, 1.3 $MgCl_2$, 2.5 $CaCl_2$, 1 NaH_2PO_4, 26.2 $NaHCO_3$, 11 glucose, pH 7.2-7.4 after CO_2 buffering, ~ 300 mosm. Additional control experiments included 10 mM BAPTA in the 10 mM $[Cl^-]_{in}$ internal solution (E_{Cl} is still -64.4 mV). Dose dependent widening of action potentials were measured at 35ºC in acute slices with physiological 10 mM $[Cl^-]_{in}$ (E_{Cl} = -64.4 mV) with 0.1, 0.3, 1, 10, 30, 100, 300, 1000 μM NFA or NPPB.

To record whole-cell NMDA-EPSCs, 3-4 MΩ recording pipettes were filled with 130 mM $[Cl^-]_{in}$ solution (mM): 10 K-gluconate, 130 KCl, 10 HEPES, 0.2 EGTA, 4 MgATP, 0.4 Na_3GTP, pH 7.2-7.4, adjusted with KOH, ~ 300 mosm. 10 mM BAPTA was added in experiments testing whether CaCC activation via NMDA-Rs was Ca^{2+} dependent. To make the 10 mM Cl^- internal solution, K-gluconate concentration was raised from 10 mM to 130 mM and KCl concentration was reduced from 130 mM to 10 mM. A zero-Mg^{2+} ACSF (without 1.3 mM Mg^{2+} but with 4

mM $CaCl_2$) was used as the external solution in order to remove Mg^{2+} block and have Ca^{2+} flux through NMDA-R activated by stimulating Schaffer collateral axons at a holding potential of -65 mV. $GABA_A$-Cl^- current was blocked with 50 µM PTX and the AMPA receptor contribution was removed with 20 µM CNQX. 100 µM APV was added at the end of the experiment to verify that NMDA receptors mediated the NMDA-EPSC recorded. Bipolar stimulation electrode was placed 100-200 µm from the CA1 pyramidal neuron cell body layer to deliver a stimulus lasting 0.1 msec every 30 seconds.

For whole-cell recording of AMPA-EPSPs, 3-4 MΩ recording pipettes were filled with 10 mM $[Cl^-]_{in}$ solution: 130 K-gluconate, 10 KCl, 10 HEPES, 0.2 EGTA, 4 MgATP, 0.4 Na_3GTP, pH 7.2-7.4, adjusted with KOH, ~ 300 mosm. ACSF was used for the external solution and included 50 µM PTX to block $GABA_A$-Cl^- channels and 100 µM APV to remove NMDA receptor contribution. For whole-cell recording of NMDA-EPSPs, 3-4 MΩ recording pipettes were filled with 10 mM $[Cl^-]_{in}$ solution: 130 K-gluconate, 10 KCl, 10 HEPES, 0.2 EGTA, 4 MgATP, 0.4 Na_3GTP, pH 7.2-7.4, adjusted with KOH, ~ 300 mosm. For 130 mM $[Cl^-]_{in}$ experiment, 130 K-gluconate concentration was reduced from 130 mM to 10 mM and KCl concentration was raised from 10 mM to 130 mM. ACSF was used for the external solution and included 50 µM PTX to block $GABA_A$-Cl^- channels and 20 µM CNQX to remove AMPA receptor contribution. 100 µM APV was added at the end of the experiment to verify that NMDA receptors mediated the NMDA-EPSP recorded. Bipolar stimulation electrode was placed 100-200 µm from the CA1 pyramidal neuron cell body layer to deliver a stimulus lasting ~ 0.1 msec every 30 seconds and input resistance was monitored throughout by applying a -5 mV hyperpolarization step with every stimulation.

To obtain field recordings, 5-10 MΩ recording pipettes were filled with ACSF and the external bath solutions contained ACSF with additional blockers of transmitter receptors. For field recording of NMDA-fEPSP, the external solution also included 50 µM PTX and 20 µM CNQX, and 100 µM D-APV was added at the end of experiment. For AMPA-fEPSP recording, the external solution also included 50 µM PTX and 100 µM D-APV, and 20 µM CNQX was added at the end of experiment. The 10 Hz stimulation was delivered with a bipolar stimulating electrode placed 100-200 microns from the recording pipette in the CA1 dendritic field.

Whole-cell recording of EPSPs, EPSP summation, and EPSP-spike coupling were done at 35ºC in acute slices and 3-4 MΩ recording pipettes were filled with 10 mM $[Cl^-]_{in}$ solution: 130 K-gluconate, 10 KCl, 10 HEPES, 0.2 EGTA, 4 MgATP, 0.4 Na_3GTP, pH 7.2-7.4, adjusted with KOH, ~ 300 mosm. For 130 mM $[Cl^-]_{in}$ experiment (E_{Cl} = 0 mV), 130 K-gluconate concentration was reduced from 130 mM to 10 mM and KCl concentration was raised from 10 mM to 130 mM. 10 mM BAPTA was added in experiments testing whether CaCC activation via NMDA-Rs was Ca^{2+} dependent. ACSF was used for the external solution and included 50 µM PTX to block $GABA_A$-Cl^- channels and 20 µM CNQX to remove AMPA receptor contribution. 20 µM CNQX and 100 µM APV were added at the end of the experiment to verify that EPSPs were mediated by glutamate receptors. 100 µM NFA was used for all synaptic potential experiments.

Bipolar stimulation electrode was place 100-200 µm from the CA1 pyramidal neuron cell body layer to deliver a stimulus lasting ~ 0.1 msec every 30 seconds. Input-output of EPSP amplitude as function of stimulus strength was constructed by using stimulus strength that gives 2 mV EPSP and normalized to that stimulus strength. Single EPSP to spike initiation threshold was determined by gradually increasing the stimulus strength for the EPSP until a single action potential was obtained;

voltage threshold was measured. 40 Hz stimulation with 3 stimuli was kept below threshold (giving a first EPSP of ~ 2 mV) to focus on EPSP summation. 40 Hz stimulation with 5 stimuli was kept just below threshold to focus on EPSP-spike coupling.

Picrotoxin (PTX), D-(-)-2-Amino-5-phosphonopentanoic acid (D-APV), tetrodotoxin (TTX), 4-aminopyridine (4AP), KN62 were purchased from Tocris (Ellisville, Missouri). Niflumic acid (NFA), 5-nitro-2-(3-phenylpropylamino)benzoic acid (NPPB), and 6-cyano-7-nitroquinoxaline-2,3-dione (CNQX) were purchased from Sigma Aldrich.

SUPPLEMENTAL TEXT

Experimental details of shRNA knockdown

As shown in Figure 4D, the knockdown is statistically significant starting 9 days post-infection. % reduction 9 days after infection: scrambled, n = 11, 16B-shRNA#2, 59 ± 4.1%, n = 9, $p < 0.01$, 16B-shRNA#5, 62 ± 5.8%, n = 8, $p < 0.01$. % reduction 10 days after infection: scrambled, n = 9, 16B-shRNA#2, 61 ± 6.8%, n = 8, $p < 0.01$, 16B-shRNA#5, 62 ± 6.5%, n = 8, $p < 0.01$.

As shown in Figure 4E, the broadening effect of shRNA knockdown of TMEM16B on action potential duration was significant starting 9 days after infection; 16B-shRNAs did not significantly alter spike threshold or amplitude. 8 days after infection: scrambled, n = 5, 16B-shRNA #2, n = 6, $p > 0.05$, 16B-shRNA #5, n = 6, $p > 0.05$. [Spike threshold: scrambled, -33.9 ± 1.11 mV (n = 5) compared to 16B-shRNA #2, -34.9 ± 0.55 mV (n = 6, $p > 0.05$) and 16B-shRNA #5, -34.3 ± 0.93 mV (n = 6, $p > 0.05$). Spike amplitude: scrambled, 114 ± 4.91 mV (n = 5) compared to shRNA #2, 113 ± 4.73 mV (n = 6, $p > 0.05$) and shRNA #5, 114 ± 3.38 mV (n = 6, $p > 0.05$)]. 9 days after infection, % increase in spike duration compared to scrambled control: scrambled, n = 11, 16B-shRNA #2, 39 ± 8.7%, n = 13, $p < 0.001$, 16B-shRNA #5, 37 ± 4.3%, n = 9, $p < 0.001$. [Spike threshold: scrambled, -34.2 ± 0.85 mV (n = 11) compared to 16B-shRNA #2, -35.7 ± 1.28 mV (n = 13, $p > 0.05$) and 16B-shRNA #5, -34.3 ± 0.66 mV (n = 9, $p > 0.05$). Spike amplitude: scrambled, 114 ± 3.44 mV (n = 11) compared to 16B-shRNA #2, 115 ± 2.31 mV (n = 13, $p > 0.05$) and 16B-shRNA #5, 113 ± 3.75 mV (n = 9, $p > 0.05$)]. 10 days after infection, % increase in spike duration compared to scrambled control: scrambled, n = 15, 16B-shRNA #2, 44 ± 6.3%, n = 13, $p < 0.001$, 16B-shRNA #5, 38 ± 6.6%, n = 15, $p < 0.001$. [Spike threshold: scrambled, -34.2 ± 1.32 mV (n = 15) compared to 16B-shRNA #2, -35.3 ± 2.31 mV (n = 13, $p > 0.05$) and 16B-shRNA #5, -34.1 ± 2.76 mV (n = 15, $p > 0.05$). Spike amplitude: scrambled, 114.6 ± 3.97 mV (n = 15) compared to 16B-shRNA #2, 114.6 ± 4.21 mV (n = 13, $p > 0.05$) and 16B-shRNA #5, 113.4 ± 5.21 mV (n = 15, $p > 0.05$)]. 12 days after infection, % increase in spike duration compared to scrambled control: scrambled, n = 11, 16B-shRNA #2, 50 ± 7.6%, n = 9, $p < 0.001$, 16B-shRNA #5, 40 ± 5.2%, n = 7, $p < 0.001$. [Spike threshold: scrambled, 34.7 ± 1.73 mV (n = 11) compared to 16B-shRNA #2, -33.7 ± 2.77 mV (n = 9, $p > 0.05$) and 16B-shRNA #5, -35.2 ± 2.91 mV (n = 7, $p > 0.05$). Spike amplitude: scrambled, 111 ± 4.87 mV (n = 11) compared to 16B-shRNA #2, 113 ± 3.18 mV (n = 9, $p > 0.05$) and 16B-shRNA #5, 112 ± 3.86 mV (n = 7, $p > 0.05$)].

As shown in Figure 6B, reducing CaCC with 100 µM NFA amplifies the larger EPSPs (from 6.17 ± 0.21 mV to 9.30 ± 0.36 mV, n = 10, $p < 0.05$) under physiological conditions when CaCC is inhibitory with 10 mM $[Cl^-]_{in}$ (E_{Cl} = -64.4 mV, left), but dampens the larger EPSPs (from 6.20 ± 0.25 mV to 4.34 ± 0.24 mV, n = 9, $p < 0.05$) when CaCC is excitatory in the presence of 130 mM $[Cl^-]_{in}$ (E_{Cl} = 0 mV, middle), and it has no effect on EPSP amplitude (from 6.21 ± 0.90 mV to 6.18 ± 0.51 mV, n = 16, $p > 0.05$) when BAPTA is included with 10 mM $[Cl^-]_{in}$ to chelate Ca^{2+} and prevent CaCC activation (right). Similar stimulation intensity and stimulator location in slice were used to elicit EPSP with small size variation (<5%) prior to NFA application; the same stimuli were used before and after NFA application. The summary plots of input-output relations involve analyses of averages of ten recordings in each condition. * $p < 0.05$.

As shown in Figure 6D, under physiological conditions when CaCC is inhibitory with 10 mM $[Cl^-]_{in}$ (E_{Cl} = -64.4 mV, left), reducing CaCC with 100 µM NFA enhances summation and increases the $3^{rd}/1^{st}$ EPSP ratio (3.19 ± 0.19 to 4.27 ± 0.42, n =8, $p < 0.01$; see Table 1). When CaCC is excitatory in the presence of 130 mM $[Cl^-]_{in}$ (E_{Cl} = 0 mV, middle), reducing CaCC with 100 µM NFA reins in EPSP summation and reduces the $3^{rd}/1^{st}$ EPSP ratio (5.04 ± 0.25 to 3.38 ± 0.18, n =9, $p < 0.01$; see Table 1). 100 µM NFA has no effect on EPSP summation when BAPTA is included with 10 mM $[Cl^-]_{in}$ to chelate Ca^{2+} and prevent CaCC activation (right) (3.30 ± 0.19 to 3.29 ± 0.17, n =5 $p > 0.05$; see Table 1).